RAMIEL: A Parallel-Wire Driven Monopedal Robot for High and Continuous Jumping

Temma Suzuki[1], Yasunori Toshimitsu[1], Yuya Nagamatsu[1], Kento Kawaharazuka[1],
Akihiro Miki[1], Yoshimoto Ribayashi[1], Masahiro Bando[1], Kunio Kojima[1],
Yohei Kakiuchi[1], Kei Okada[1], and Masayuki Inaba[1]

Abstract— Legged robots with high locomotive performance have been extensively studied, and various leg structures have been proposed. Especially, a leg structure that can achieve both continuous and high jumps is advantageous for moving around in a three-dimensional environment. In this study, we propose a parallel wire-driven leg structure, which has one DoF of linear motion and two DoFs of rotation and is controlled by six wires, as a structure that can achieve both continuous jumping and high jumping. The proposed structure can simultaneously achieve high controllability on each DoF, long acceleration distance and high power required for jumping. In order to verify the jumping performance of the parallel wire-driven leg structure, we have developed a parallel wire-driven monopedal robot, RAMIEL. RAMIEL is equipped with quasi-direct drive, high power wire winding mechanisms and a lightweight leg, and can achieve a maximum jumping height of 1.6 m and a maximum of seven continuous jumps.

I. INTRODUCTION

Legged robots have a higher ability to overcome discrete footholds and steps than wheeled robots, and are expected to be applied to transportation of goods and patrolling. In particular, legged robots that can jump are being actively researched because they can move over more three-dimensional terrain [1]–[6].

Several leg robots, [5], [6], have been developed so far that can perform a single jump with a CoG (center of gravity) jump height of 3 m (the CoG jump height is the difference between the height of the CoG at the moment the foot leaves the ground and at the highest point during the jump). On the other hand, robots that specialize in single high jump are not equipped with actuators necessary for posture control and adjustment of the next leg position in order to reduce the weight of the machine. As a result, it is difficult for them to move with continuous jumps. In addition, it is predicted that the weight of the robot will increase significantly and the jumping height will decrease if the actuator for posture control is installed in the legged robot specialized for single high jumping.

Legged robots that can continuously jump and locomote have been developed, such as ATLAS [3], which achieves dynamic motions such as parkour using hydraulic drive, and Salto-1P [1], which achieves a jump of 1 m by combining
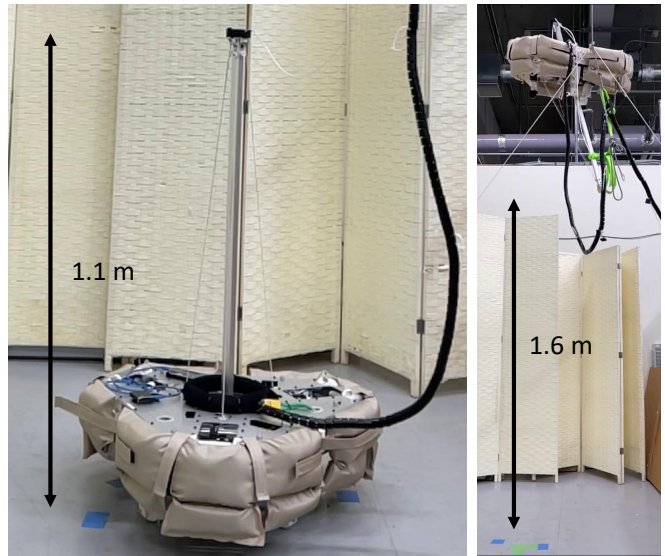

Fig. 1. Overview of the parallel wire-driven leg and snapshot of 1.6 m high jumping motion.

an electric motor, series elastic elements, and an optimized link structure. On the other hand, these continuous jumping robots have a maximum CoG jumping height of 1.1 m, which is lower than that of legged robots specialized for single jumping [1], [2]. (For the previous study [1], [2], which used the difference between the height of the CoG in a bent position and the height of the CoG at the highest point during a jump as the index of the jump height, the CoG was calculated by subtracting the leg stroke from the jump height described in the papers).

Therefore, the purpose of this study is to clarify the leg structure that can achieve both continuous jumping and high jumping. As a leg structure to achieve this purpose, we propose a parallel wire-driven leg structure as shown in Fig. 1, in which a leg with one DoF of linear motion and two DoFs of rotation is controlled by six wires.

In Section II, we explain the parallel wire-driven leg structure and compare its jumping performance with that of existing leg structures. In Section III, we describe the overall design of RAMIEL, a monopedal robot developed to verify the jumping performance of the parallel wire-driven leg structure and the detailed design of the wire winding mechanism. In Section IV, we describe the hopping controller of RAMIEL. In Section V, we perform continuous

[1] The authors are with the Department of Mechano-Informatics, Graduate School of Information Science and Technology, The University of Tokyo, 7-3-1 Hongo, Bunkyo-ku, Tokyo, 113-8656, Japan. [suzuki, toshimitsu, nagamatsu, kawaharazuka, miki, ribayashi, bando, kojima, kakiuchi, okada, inaba]@jsk.t.u-tokyo.ac.jp
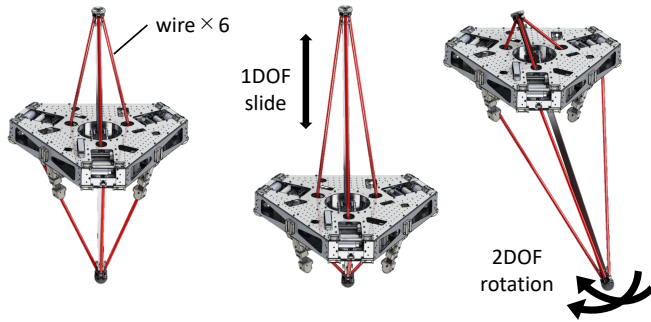
Fig. 2.   Structure of the parallel wire-driven leg.

jumping and high jumping experiments using RAMIEL and discuss the results of the experiments. In Section VI, we discuss the jumping performance of the parallel wire-driven leg structure based on the experimental results.

II. STRUCTURE AND ADVANTAGES OF PARALLEL WIRE-DRIVEN LEG

A. Structure of Parallel Wire-driven Leg

The parallel wire-driven leg structure is shown in Fig. 2. The parallel wire-driven leg structure consists of a body part and a leg part which has one DoF of linear motion and two DoFs of rotation relative to the body part. The joints of the leg are controlled by six wires extending from the main body. Each wire is wound by an independent electric motor, and the target leg posture is realized by adjusting the winding length of the wire.

A robot with a similar structure is FALCON [7]. However, FALCON is a robot designed for manipulation tasks whose body is fixed to the environment, and its design requirements are quite different from those of the legged robots that realize continuous jumping and high jumps.

B. Advantages of Parallel Wire-driven Leg in Jumping

In order for a legged robot to perform high jumps, the following three conditions must be met.

1) The force to lift the robot must be high.
2) The acceleration distance must be large.
3) The vertical velocity must not saturate during acceleration.

Since the legged robot cannot accelerate vertically in the air, the jump height is uniquely determined from the vertical velocity at takeoff. In other words, to increase the jump height, we need to increase the velocity at take-off. In order to increase the velocity at takeoff, the acceleration of the robot must be large (the force to lift the robot must be large), and the acceleration distance must be large. In addition, the saturation of the output speed of the actuator must be considered. In an electric motor, as the angular velocity of the output axis increases, the back electromotive force also increases, so the angular velocity saturates at a certain value and further acceleration is not possible. Since actuators generally have such a maximum speed, it is also required that the actuator speed does not saturate during acceleration

(vertical velocity must not saturate during acceleration) in order to increase the velocity at takeoff.

In the animal-like rotational joint leg structure [3], [8], which is adopted by many legged robots, there is a trade-off between condition 2 (extension of acceleration distance) and condition 3 (prevention of velocity saturation). In the case of the leg that uses the rotational joint for vertical acceleration, it is necessary to take off with the knee extended in order to satisfy the condition 2. However, in the rotational joint leg structure, the more the knee is extended, the closer the leg is to the singularity, and the vertical velocity approaches zero. Therefore, in order to satisfy the condition 3, it is necessary to take off with the knee bent to some extent. This problem also occurs in legs with a special parallel link structure of non-animal type, such as the GOAT [9], if they are rotational joint legs. Thus, in the rotational joint leg structure, conditions 2 and 3 are contradictory, and the high jump is hindered.

On the other hand, the parallel wire-driven leg structure does not have such conflict in conditions 2 and 3 as the rotating joint leg structure, and can satisfy the three conditions more easily. In the parallel wire-driven leg structure, the vertical speed does not decrease even when the leg is extended because the linear joint is used for vertical acceleration. Therefore, it is possible to accelerate with the maximum range of motion. In addition, the parallel wire-driven leg structure can lift the body by using three motors in parallel, which can easily satisfy the condition 1 compared with the leg structure using actuators in series [3], [8].

Finally, we confirm the conditions required for the leg structure to perform continuous jumping. For continuous jumping, it is important that the leg is light. In continuous jumping, the robot moves its leg quickly to stabilize its posture. If the leg is heavy, the maximum acceleration of the leg is reduced and the posture of the main body easily collapses due to the recoil of the leg. The parallel wire-driven leg structure realizes a lightweight leg without any actuators and enables the robot to move the leg agilely.

The advantages of the parallel wire-driven leg structure in high jumps and continuous jumps have been described, but one of the disadvantages of the parallel wire-driven leg structure is that its self weight must be supported only by the actuator force. In the case of a leg with rotational joints, such as in animals, it is possible to support most of the self weight by extending the knee joint. On the other hand, parallel wire-driven legs have a disadvantage that they cannot support their own weight with their joints because they use vertical linear joints, and thus consume a lot of power just to keep standing. This disadvantage is the reverse of the advantage that the vertical velocity does not decrease even when the knees are extended, and is considered to be the result of specializing in jumping at the expense of power consumption.
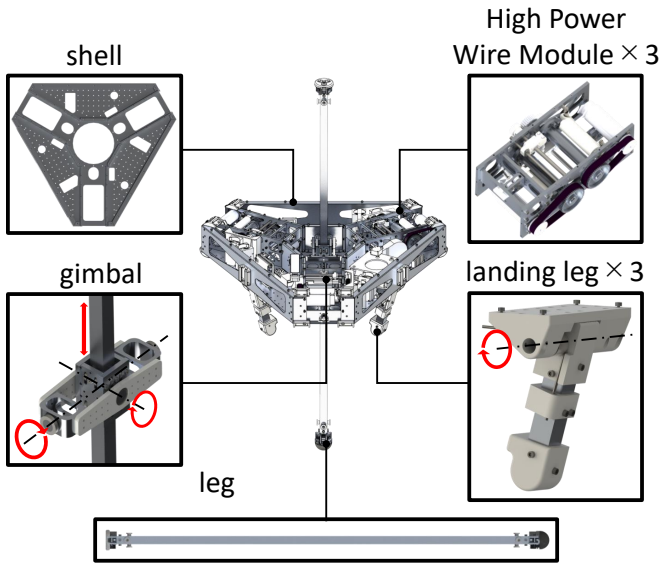
shell

gimbal

leg

High Power
Wire Module × 3

landing leg × 3

Fig. 3.   Detailed design of RAMIEL.

TABLE I
PHYSICAL PARAMETERS OF RAMIEL.

Parameter	Value
Overall height	1.07 m
Overall width	0.55 m
Total mass (body and leg)	10.3 kg
Body mass	9.8 kg
Leg mass	0.5 kg
Body moment of inertia	0.225 kg m^2
Leg moment of inertia	0.074 kg m^2
Slide joint stroke	0.8 m
Roll joint movable range	-0.79 rad to 0.79 rad
Pitch joint movable range	-0.79 rad to 0.79 rad
Maximum wire tension	230 N at 50 A
Maximum force of leg slide joint	690 N
Maximum speed of leg slide joint at no load	15 m/s at 70 V

III. DESIGN OF PARALLEL WIRE-DRIVEN MONOPEDAL ROBOT

A. Overview of Parallel Wire-driven Monopedal Robot

To verify the jumping performance of the parallel wire-driven leg structure, we have designed and built a monopedal robot RAMIEL (pa**RA**llel wire-driven **M**onopedal ag**I**l**E** **L**eg). The details of RAMIEL are shown in Fig. 3. In addition, the specifications of RAMIEL are shown in Table I. RAMIEL is a robot with a height of 1.07 m, a width of 0.55 m, and a weight of 9.8 kg. RAMIEL can be roughly divided into two parts: the leg and the body. In order to increase the efficiency of the experiment, the power supply is installed outside.

In order to achieve high and continuous jumps, the leg has a lightweight structure consisting of only an aluminum square hollow pipe, wire attachment parts, and rubber for ground contact. The leg has a simple configuration without actuators, which makes it light and controllable.

The body part consists of an outer shell as the frame, a gimbal module connecting the body and the leg, landing legs as grounding points when the body touches the ground, and High Power Wire Modules controlling the wires. The detailed design of the wire module is described in the next section. The outer shell is a monocoque structure made of aluminum with thicknesses of 1 mm and 1.5 mm, which is both lightweight and rigid. In addition, cushions are installed on the surface of the outer shell to protect the contents when the side of the body part comes into contact with the ground. The cushions are a simplified version of the pneumatic damper shock-absorbing outer shell [10] developed by Takeda et al. In Takeda et al.'s method, a hole of about 10 mm in diameter was drilled in the surface of the cushion, and the damper function was realized by viscously releasing air through the hole when the cushion was impacted. On the other hand, the cushions installed in RAMIEL have no air holes on its surface, and air leaks out through the seams of the fabric to realize the damper function more simply.

The gimbal has one DoF for rotation in the roll and pitch axes, respectively, and one Dof for linear motion parallel to pipe of the leg. The linear motion mechanism is realized by pressing the square pipe of the leg from all sides with bearings attached to the inner wall of the gimbal. The gimbal does not have any actuators or sensors, and has a simple and robust structure.

The landing legs enable RAMIEL to start jumping from the ground and to return to the landing state after the completion of the jumping motion. The landing leg has a rotational DoF at the base, and is almost vertical to the ground by the built-in torsion spring in the normal state. When RAMIEL collides with the ground at an angle, the landing legs are folded from the base to absorb the impact.

B. Design of High Power Wire Module

RAMIEL uses six wires to control the posture of the leg and is equipped with three sets of modules to control the length of the wires. One wire module controls the winding length of two wires independently. The details of the High Power Wire Module installed in RAMIEL are shown in Fig. 4. The wire module must satisfy the following three conditions to achieve high and continuous jumps.

1) Tension and maximum velocity are large enough for jumping.
2) Will not be destroyed by the impact of landing.
3) Be able to wind the wire exactly to the intended length.

In this study, a High Power Wire Module is developed to meet these three requirements. In the following, we review these three requirements in detail and explain how the wire module satisfies them.

First, both the maximum winding speed and the maximum tension of the wire must be sufficiently high to achieve a high jump. The High Power Wire Module satisfies this requirement by operating BLDC motors (Maxon [11]) that winds the wire under the high-power conditions of input voltage 70 V and maximum instantaneous current 50 A [12]. The output shaft of the motor is reduced to 2.5/1 by a timing pulley and input to a wire winding pulley with a diameter of 20 mm. The maximum tension of the wires is about 230 N
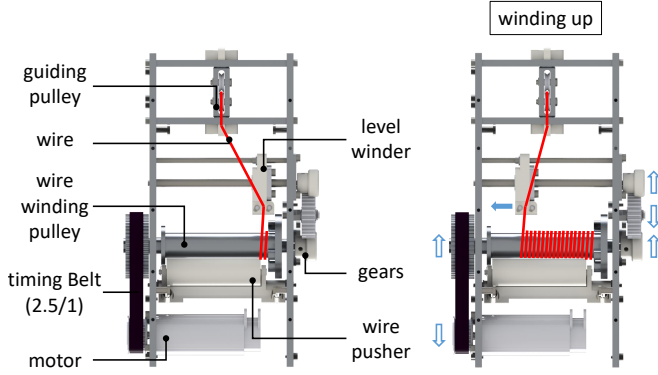
Fig. 4. Detailed design of High Power Wire Module.

(50 A is applied), and approximating the parallel wire-driven leg structure as a simple linear motion, the three wires can lift the robot body with a total force of 690 N. This means that RAMIEL can be accelerated at six times the gravitional acceleration. In addition, the high input voltage of the motor, 70 V, allows the maximum wire winding speed to be as fast as 10.7 m/sec even with a high current of 50 A. Assuming that the parallel wire-driven leg structure is approximated as a simple linear motion and the robot is ejected vertically upward at 10.7 m/sec, the robot can theoretically jump to a height of about 5.8 m.

Secondly, a major problem for a jumping robot is that a large impact on landing can destroy the leg and actuators. In the High Power Wire Module, the reduction ratio of the motor is set to be as low as 2.5/1 and the quasi-direct drive is adopted to solve this problem. The quasi-direct drive causes the wire to backdrive when landing, reducing the impact on the leg and actuators.

Thirdly, for accurate posture control of the leg in continuous jumping, it is necessary to wind the wire precisely for the intended length. In the High Power Wire Module, a level winder and a wire pusher are used to achieve accurate wire winding. The wire from the wire winding pulley passes through the level winder to the guiding pulley. The level winder moves linearly on the sliding screw in conjunction with the rotation of the wire winding pulley, and plays the role of aligning the wire on the winding pulley. The wire puhser prevents the wire from crossing each other on the winding pulley and assists smooth winding. The wire has a diameter of 2 mm with a zylon® core yarn and polyester side yarns, and the wire elongation is considered to have a small effect on the winding length because the wire elongation is only about 1 % even when the maximum tension of the wire module of 230 N is applied.

IV. CONTROLLER OF PARALLEL WIRE-DRIVEN MONOPEDAL ROBOT

In this section, we describe the controller for RAMIEL's hopping operation, which is based on the controller of the 3D One-Legged Hopping Machine of Raibert et al. with modifications to support a parallel wire-driven leg strcture [13].

Fig. 5 shows an overview of the controller. The controller assumes that the motion in the pitch and roll directions (in the XZ and YZ planes, respectively) are decoupled from each other, so the same processing is performed for each direction. Therefore, for simplicity, the following explanation is limited to the pitch direction, i.e., the XZ plane.

The inputs of the controller are the wire length l and velocity $\dot{l}$ obtained from the encoders of each motor, the acceleration a and angular velocity ω obtained from the IMU fixed to the body part, and the estimated velocity v of the body part as a result of visual-inertial odometry performed by the RealSense T265. In addition, a Magdwick filter is used to estimate the rotational posture R from the IMU sensor information [14]. Since the joint does not have a built-in encoder, the joint posture is estimated from the wire length and velocity using the Extended Kalman Filter (EKF).

The EKF is constructed as follows. First, the state x to be estimated is defined from the joint position q and the joint velocity $\dot{q}$, and the observed value z is defined as a vector consisting of the wire length l and the wire velocity $\dot{l}$ as follows.

$$x = \begin{bmatrix} q \\ \dot{q} \end{bmatrix} \in \mathbb{R}^6 \quad z = \begin{bmatrix} l \\ \dot{l} \end{bmatrix} \in \mathbb{R}^{12} \quad (1)$$

The state transition model can then be defined as follows.

$$x_{i+1} = \begin{bmatrix} I & Idt \\ O & I \end{bmatrix} x_i + w \quad (2)$$

where the subscript i denotes the data at step i, I is the unit matrix, O is the zero matrix, dt is the time step of the state transition, and w is the noise of the model. The observation model can be defined as follows.

$$z_i = h(x_i) + v$$
$$h(x_i) := \begin{bmatrix} g(q_i) \\ J_m(q_i)\dot{q}_i \end{bmatrix} \quad (3)$$

The model is nonlinear. Here, $g(\cdot)$ and $J_m(\cdot)$ are functions that calculate the wire length and muscle jacobian from the joint position, respectively. $g(\cdot)$ is a function that calculates the wire path by geometric calculation based on the dimensional information of the CAD model, and its analytical partial differentiation is used as $J_m(\cdot)$ [15]. The lower wires tended to become slack upon landing, as they are quickly shortened while carrying little tension. This results in an error of the joint angle output from the EKF, and to prevent this the measurements of the lower wires were weighted to have less effect on the estimation for 0.1 s after touchdown was detected.

In the control of the hopping motion, the joint force $\tau \in \mathbb{R}^3$, which is a combination of the torque of the rotary joint and the force of the linear joint, is output, and it is converted to the wire tension f before being sent to the wire module of the robot. The conversion from τ to f is done using computed muscle control, which can be formulated
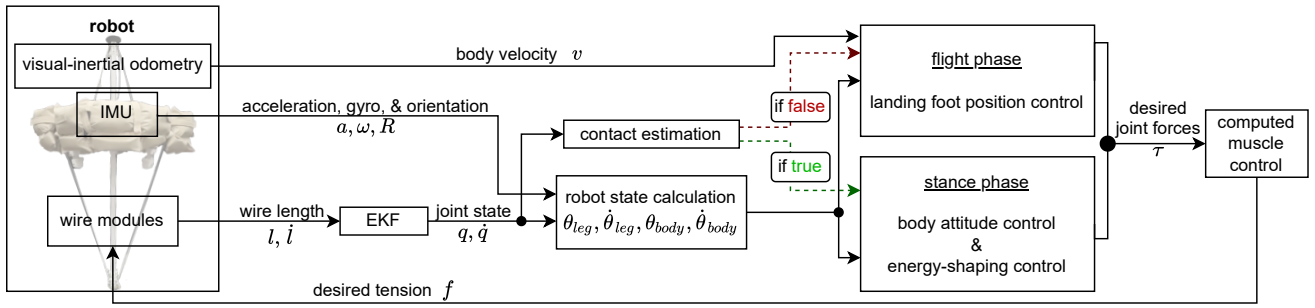
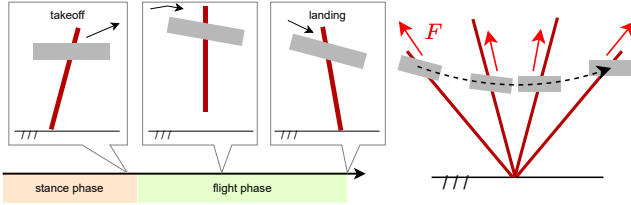Fig. 5. Overview of the hopping controller.

Fig. 6. Phases of hopping.

Fig. 7. Force encountered during stance phase.

as a quadratic programming (QP) method using the muscle jacobian J_m as follows [16], [17].

$$
\begin{aligned}
&\underset{\boldsymbol{f}}{\arg\min} \quad ||\boldsymbol{f}||^2 \\
&\text{subject to} \begin{cases} \boldsymbol{\tau} = -J_m^T \boldsymbol{f} \\ \boldsymbol{f} \geq \boldsymbol{f}_{min} \end{cases}
\end{aligned}
\tag{4}
$$

$||\cdot||^2$ denotes the L2 norm, and $\boldsymbol{f}_{min}$ denotes the minimum tension required to keep the wire taut.

As shown in Fig. 6, the hopping motion can be divided into a stance phase, in which the feet are touching the ground, and a flight phase, in which the feet are away from the ground. At the moment of transition to the stance phase, i.e., at the time of landing, the robot has a vertical downward velocity component and a horizontal velocity component. After that, as shown in Fig. 7, the robot sinks and rises like a spring throughout the stance phase, and enters the flight phase when the normal force against the ground becomes zero. In the flight phase, the motion changes with an acceleration of $-g$ in the vertical direction.

In the stance phase, PD control is applied to the rotational joints so that the posture of the body is horizontal. For the linear motion direction, the summed force of a constant feed-forward element F_F and a feedback element F_B are generated to accelerate the body upward. The feedback element F_B is determined by the energy shaping control law as shown in the following equation, depending on the difference between the target and actual mechanical energy to maintain an appropriate hopping height.

$$
\begin{aligned}
F_B(x,\dot{x}) &= k_E(E_{des} - E(x,\dot{x}))\dot{x} \\
E_{des} &:= \frac{1}{2}m_B\dot{x}_{des}^2 \\
E(x,\dot{x}) &:= \frac{1}{2}m_B\dot{x}^2 + F_F x - m_B g(x-x_0)
\end{aligned}
\tag{5}
$$

Here, x is the linear joint position, k_E is the feedback gain, m_B is the mass of the body, and g is the gravitational acceleration. The E_{des} is the target value of the mechanical energy, which in the above equation is determined from the vertical velocity $\dot{x}_{des}$ during takeoff, but it can also be determined from the target hopping height.

During the flight phase, the robot should maintain a constant position x_0 for the linear joint so that the length of the leg does not change. In the rotational direction, based on the horizontal velocity v_H of the robot, the target foot position p_0 is determined by the following feedback law, which is a simplified version of the control law [13] of Raibert et al., to keep it hopping in place.

$$
p_0 = k v_H
\tag{6}
$$

Here, k is the gain, and after obtaining a stable value on the simulator, we manually adjusted it to be stable on the actual machine. The horizontal velocity v_H was obtained from the visual inertial odometry output from the RealSense T265 attached to the robot body.

The controller judges that it is the flight phase if the position of the linear joint is closer to x_0 than the threshold value, and the stance phase otherwise.

Finally, the process at the beginning and end of the hopping motion is described. At the start of the hopping motion, the robot is grounded on the landing leg as shown in Fig. 8. Then, after applying a force to accelerate the robot upward in the linear direction for a certain period of time, the ascent speed is adjusted by the feedback law of Eq. 5 until the transition to the stance phase, and the robot jumps up at the target speed. After completing the hopping motion, the robot returns to ground contact with the landing leg, which was achieved by setting a large D gain to decelerate against the linear motion direction.
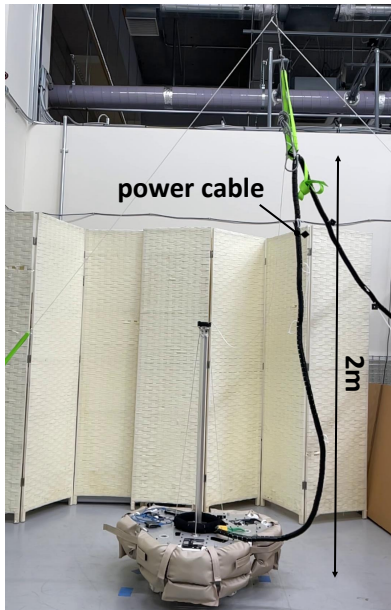
Fig. 8. Initial state of RAMIEL in the jumping experiments.

V. Experiments

A. Experimental Condition

In this chapter, we perform high jump experiments and continuous jump experiments using RAMIEL, and discuss the results of each experiment. The experimental setup is shown in Fig. 8. All experiments are performed on a horizontal floor. The power to drive the motor and the control circuit of RAMIEL are both supplied from outside through cables. The power cable extending from RAMIEL is suspended from a height of 2 m.

As mentioned earlier, RAMIEL is not equipped with an encoder to read the joint angle directly, and the joint angle is estimated from the displacement of the wire length. The initial value for joint angle estimation was set as follows. First, the joint is fixed to a known joint angle using a jig. Next, the wire is wound with a small tension of 0.5 N. The initial length is set to the wire winding length when the wire is no longer loose. During the jump, the difference between the initial length and the current wire length is used to estimate the current joint angle.

B. High Jump

First, we perform a jumping experiment with a commanded CoG jump height of 1 m. RAMIEL during the jump is shown in Fig. 9. It can be seen that the body of RAMIEL jumps from the horizontal ground position and returns to the starting position after the jump. The vertical displacement of the CoG of RAMIEL is shown in Fig. 10. The height of the CoG of RAMIEL at takeoff is 0.9 m, and the maximum height is 1.63 m, indicating that the CoG of RAMIEL is displaced vertically by a maximum of 0.73 m. The vertical displacement of the CoG in the jump experiment with the commanded jump height of 1 m was measured using motion capture.

Next, we will perform a jumping experiment with the commanded jump height of the CoG 2 m. RAMIEL during

the jump is shown in Fig. 11. It can be seen that the jump is successful, but the landing is not. In addition, while the robot is in the air, one of the upper wires snapped and the other wires became loose. The vertical displacement of the CoG of RAMIEL is shown in Fig. 12. The vertical displacement of the CoG is measured using an RealSense T265 attached to RAMIEL body, because RAMIEL exceed the view of the motion capture system in the jumping experiment of the commanded CoG jump height 2 m. Since the CoG is measured using RealSense, there is an offset in the height of the CoG compared to that using motion capture. Since the CoG jump height is the difference between the CoG height at the moment when the foot leaves the ground and the CoG height at the heighest point, the same CoG jump height is measured by both RealSense and motion capture regardless of the offset of the CoG height. Therefore, the same CoG jump height is measured by both RealSense and motion capture regardless of the offset. The height of the CoG of RAMIEL at takeoff was 0.57 m, and the maximum height was 2.16 m, indicating that the CoG of RAMIEL was displaced vertically by a maximum of 1.59 m.

We discuss the results of these experiments. The experimental results for the commanded CoG jump height 2 m show that the parallel-wire monopedal robot is capable of achieving the force and velocity required for a jump of 1.6 m. This value of 1.6 m is 1.45 times higher than the maximum CoG jump height 1.1 m [1], [2] of existing leg robots capable of controlled continuous jumping. Furthermore, in order to match the conditions of comparison with the robots that achieved the maximum CoG jump height 1.1 m [1], [2], we consider installing a battery in RAMIEL to power it internally, The total weight is expected to increase from 10 kg to 12.5 kg [1]. If the weight of RAMIEL is increased by a factor of 1.25, the CoG jump height is predicted to be 1.44 m based on the law of conservation of energy, which is also higher than the maximum CoG jump height 1.1 m of existing leg robots capable of continuous jumping. It is possible that the internal power supply will increase the drop of the power supply voltage at the time of jumping, and the jumping height may be lower than this prediction. However, as described in the Subsection III-B, the theoretical CoG jump height is 5.8 m when the maximum current of 50 A is applied to the motor at the power supply voltage 70 V. Therefore, it can be inferred that CoG jump height 1.44 m is feasible even with a slight drop in the power supply voltage.

In the experiment with the commanded CoG jump height of 1 m, the robot successfully landed from the height of 0.7 m without any damage, which confirms the high impact resistance of the parallel wire-driven leg structure due to the lightness of the leg and the back-drivability of the wire.

On the other hand, the actual jumping height was lower than the commanded CoG jumping height by 0.3 m-0.4 m. This is thought to be caused by the fact that the actual tension is lower than the commanded tension due to the friction

---

[1]Three LiPo batteries for motor (6s, 0.5 kg), one LiPo battery for circuit power (3s, 0.25 kg), and power supply circuit (0.75 kg) for total 2.5 kg
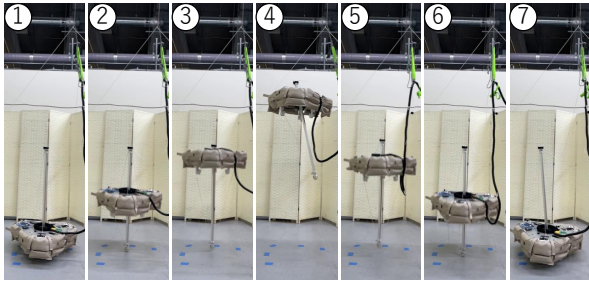
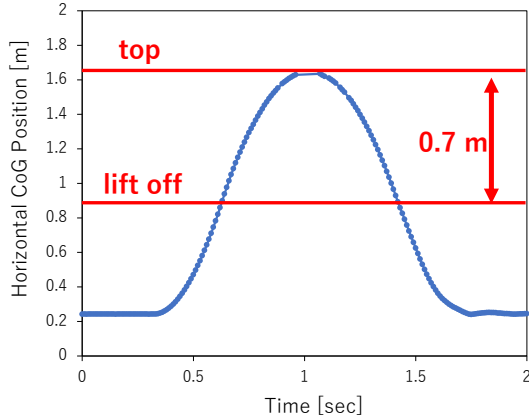Fig. 9. Snapshots of 0.7 m high jumping motion. RAMIEL can jump and land from seated position.

Fig. 11. Snapshots of 1.6 m high jumping motion. RAMIEL fails to land.

Fig. 10. Vertical position of RAMIEL's center of gravity (CoG) during a jump of 0.7 m in height.
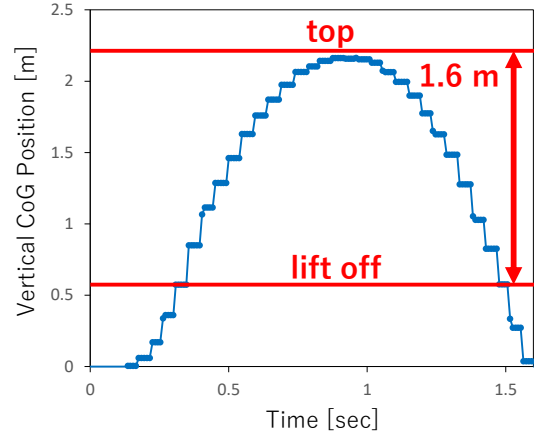
Fig. 12. Vertical position of RAMIEL's center of gravity (CoG) during a jump of 1.6 m in height.

between the wire and the transit point in the wire module. As a countermeasure to the wire friction, the bearing with which the wire comes into contact can be replaced with one with a larger outer diameter. In the experiment with a commanded CoG jump height of 2 m, the wire was cut in midair. This is thought to be caused by repeated contact between the wire and the edge of some part of the leg. The countermeasures against wire breakage include fillet the parts that the wire may contact and protect the wire with a bellows-like cover.

C. Continuous Jump

In this section, we perform continuous jumping experiments using RAMIEL. In this experiment, the CoG of RAMIEL is measured by using RealSense T265 installed in RAMIEL itself.

The results of 16 trials for continuous jumping experiments with the same control parameters and environment are summarized in Table II. In 5 of these trials, the robot succeeded in jumping more than 5 consecutive times (The number of times the leg left the ground is considered to be the number of continuous jumps). The results of the 14th jump experiment are shown in Fig. 13. The position of the CoG of RAMIEL during the experiment is shown in Fig. 14. From these figures, it can be confirmed that RAMIEL made seven continuous jumps from the seated state and returned to the seated state after landing. These experimental results
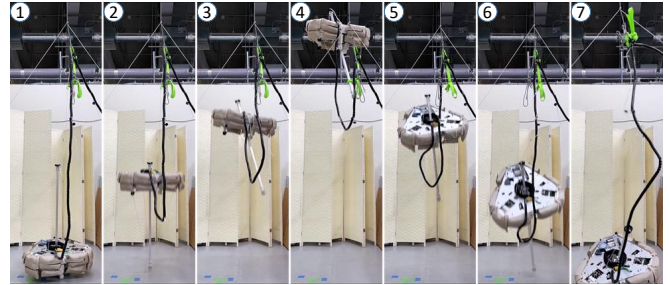
show that the parallel wire-driven leg structure has high controllability of the leg required for continuous jumping.

On the other hand, in nine out of fifteen experiments, the number of continuous jumps ended at two. In these experiments, the leg was tilted so much in the first stance that they gained horizontal speed, and in the second stance, the leg was tilted so much that they exceeded the range of motion of the joints. One of the causes of such falls is that the power cable contacts RAMIEL and generates a disturbance force. It is expected that the stability of the robot can be improved by installing a battery in the robot to eliminate the disturbance of the power cable and by adding an ankle to increase the DoF of the control.

VI. Conclusion

In this study, we proposed a parallel wire-driven leg structure in order to clarify the leg structure which can realize continuous jumping and high jumping. The parallel wire-driven leg structure has DoFs for posture control, which enable continuous jumping, and the linear motion joint is more advantageous for high jumping than the rotary joint. We developed a parallel-wire monopedal robot, RAMIEL, which has both the important conditions for high jumping, i.e., high velocity at take-off, and the important condition for continuous jumping, i.e., light weight leg. Furthermore, we have achieved a CoG jump height of 1.6 m and a

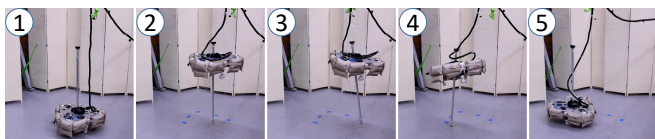| Trial	1	2	3	4	5	6	7	8	9	10	11	12	13	14	15	16
Number of continuous jumps	2	2	2	3	8	5	2	2	2	2	6	2	0	7	2	6

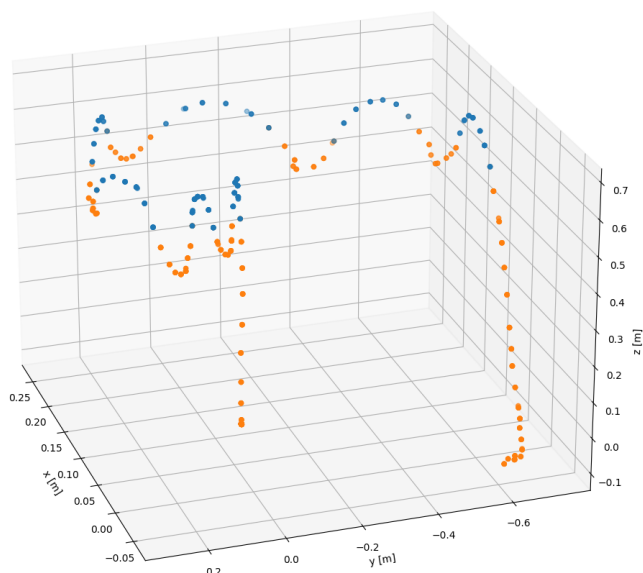Fig. 13. Snapshots of 7 continuous jumping motion. RAMIEL can jump and land from seated position.

Fig. 14. Position of RAMIEL's center of gravity (CoG) during 7 continuous jumping motion. Stance phases are shown in orange. Flight phases are shown in blue.

maximum of seven continuous jumps with RAMIEL. From these experiments, we concluded that the parallel wire-driven leg structure can realize continuous jumps and high jumps.

In the future, we will add an encoder to each joint to improve the accuracy of joint angle estimation and add an ankle to control the posture of the leg during stance.

REFERENCES

[1] D. W. Haldane, J. K. Yim, and R. S. Fearing, "Repetitive extreme-acceleration (14-g) spatial jumping with salto-1p," in *Proceedings of the 2017 IEEE/RSJ International Conference on Intelligent Robots and Systems*, 2017, pp. 3345–3351.

[2] N. Kau, A. Schultz, N. Ferrante, and P. Slade, "Stanford doggo: An open-source, quasi-direct-drive quadruped," in *Proceedings of the 2019 IEEE International Conference on Robotics and Automation*, 2019, pp. 6309–6315.

[3] "ATLAS (Bostoon Dynamics)." https://www.bostondynamics.com/atlas.

[4] P. Arm, R. Zenkl, P. Barton, L. Beglinger, A. Dietsche, L. Ferrazzini, E. Hampp, J. Hinder, C. Huber, D. Schaufelberger, *et al.*, "Spacebok: A dynamic legged robot for space exploration," in *Proceedings of the 2019 IEEE International Conference on Robotics and Automation*, 2019, pp. 6288–6294.

[5] V. Zaitsev, O. Gvirsman, U. B. Hanan, A. Weiss, A. Ayali, and G. Kosa, "A locust-inspired miniature jumping robot," *Bioinspiration & Biomimetics*, vol. 10, no. 6, p. 066012, 2015.

[6] M. A. Woodward and M. Sitti, "Multimo-bat: A biologically inspired integrated jumpinggliding robot," *The International Journal of Robotics Research*, vol. 33, no. 12, pp. 1511–1529, 2014.

[7] S. Kawamura, W. Choe, S. Tanaka, and H. Kino, "Development of an ultrahigh speed robot falcon using parallel wire drive systems," *Journal of the Robotics Society of Japan*, vol. 15, no. 1, pp. 82–89, 1997.

[8] G. Bledt, M. J. Powell, B. Katz, J. D. Carlo, P. M. Wensing, and S. Kim, "MIT Cheetah 3: Design and Control of a Robust, Dynamic Quadruped Robot," in *Proceedings of the 2018 IEEE/RSJ International Conference on Intelligent Robots and Systems*, 2018, pp. 2245–2252.

[9] S. Kalouche, "Goat: A legged robot with 3d agility and virtual compliance," pp. 4110–4117, 2017.

[10] H. Takeda, Y. Kakiuchi, S. Noda, K. Kojima, M. Bando, H. Sugai, K. Okada, and M. Inaba, "Ukemi motion for a life-size humanoid with the air damper shock absorbing exteriors," 2019, pp. 3L3–01.

[11] "Maxon," https://www.maxon.net/en/.

[12] F. Sugai, K. Kojima, Y. Kakiuchi, K. Okada, and M. Inaba, "Design of tiny high-power motor driver without liquid cooling for humanoid jaxon," in *Proceedings of the 2018 IEEE-RAS International Conference on Humanoid Robots*, 2018, pp. 1059–1066.

[13] M. H. Raibert, J. H. Benjamin Brown, and M. Chepponis, "Experiments in balance with a 3d one-legged hopping machine," *The International Journal of Robotics Research*, vol. 3, no. 2, pp. 75–92, 1984.

[14] S. Madgwick, "An efficient orientation filter for inertial and inertial/magnetic sensor arrays," *Report x-io and University of Bristol (UK)*, vol. 25, pp. 113–118, 2010.

[15] "autodiff," https://autodiff.github.io, 2022 [Online].

[16] M. Jäntsch, S. Wittmeier, K. Dalamagkidis, A. Panos, F. Volkart, and A. Knoll, "Anthrob - A Printed Anthropomimetic Robot," in *Proceedings of the 2013 IEEE-RAS International Conference on Humanoid Robots*, 2013, pp. 342–347.

[17] M. Kawamura, S. Ookubo, Y. Asano, T. Kozuki, K. Okada, and M. Inaba, "A joint-space controller based on redundant muscle tension for multiple dof joints in musculoskeletal humanoids," in *Proceedings of the 2016 IEEE-RAS International Conference on Humanoid Robots*, 2016, pp. 814–819.